FEM STUDY OF SYNCHRONIZATION BETWEEN PULSES AND TOOL OSCILLATIONS AT ULTRASONIC AIDED MICROELECTRODISCHARGE MACHINING

Daniel GHICULESCU[1], **Niculae-Ion MARINESCU**[2], **Sergiu NANU**[3],
Daniela GHICULESCU[4], **George KAKARELIDIS**[5]
[1] "Politehnica" University of Bucharest, Romania, daniel.ghiculescu@nsn.pub.ro
[2] "Politehnica" University of Bucharest, Romania, niculae.marinescu@nsn.pub.ro
[3] "Politehnica" University of Bucharest, Romania, sergiu.nanu@nsn.pub.ro
[4] National Authority for Scientific Research, Romania, daniela.ghiculescu@ancs.ro
[5] Technological Educational Institute of Patras, Greece, gkakarel@gmail.com

Abstract: The paper deals with study through Finite Element Method (FEM) of synchronization between pulses and tool oscillations at ultrasonics (US) aided micro-Electrodischarge Machining (μEDM) aiming at increasing the machining rate and the surface quality. These main output technological parameters at μEDM are not as good as they are expected due to instability of material removal process and long duration of gas bubble formed around plasma channel. The ultrasonic longitudinal oscillations of electrode-tool produce cavitation within frontal working gap leading to collective implosion of gas bubbles. This hydraulic phenomenon can remove the workpiece material in solid or plastic state or even in liquid state if synchronization between EDM pulse end and US stretching semiperiod oscillation end is achieved. The range of time interval between those critical moments is determined by FEM.

Keywords: electrodischarge machining, ultrasonics, synchronization.

1. INTRODUCTION

The micro-Electrodischarge Machining (μEDM) is characterized by very narrow working gap, less than 10 μm and therefore instability of the machining process occurs due to difficult evacuation of the removed particles. Under these conditions, machining rate is very low and surface quality is damaged by frequent short-circuits [1]. Moreover the life duration of gas bubble formed around plasma channel at μEDM is very long after pulse end, contributing to low efficiency of the removal process [2]. Among several solutions to increase the μEDM performances, the ultrasonic aiding (μEDM+US) is very effective [3], [4] when the fabrication volume is large enough to justify the corresponding additional expenses and the long manufacturing preparation.

Nevertheless some optimization conditions of working parameters are needed to attain the expected performances of μEDM+US - increasing with more than 400% machining rate (V_W) and decreasing with 50% surface R_a roughness against classic μEDM [5]. The synchronization between the pulses provided by EDM generator and ultrasonic longitudinal oscillations of electrode-tool produced by US generator is necessary in order to take maximum advantage of cavitation ultrasonically induced within the frontal working gap. The collective implosion of gas bubbles occurs only after dielectric liquid stretching semiperiod, which must be produced shortly after the pulse end.

In order to evaluate this time interval between pulse end and ultrasonic implosion, Comsol Multiphysics, Transient Heat Transfer Module was used for thermal phenomena modelling, specific to EDM. Several temperature distributions were achieved in order to simulate the critical moments of discharges against the bubbles collective implosion ultrasonically induced.

2. PHENOMENOLOGY

The gas bubble duration formed around plasma channel during discharge is critical in terms of removed volume from the workpiece, because only after its implosion the hydraulic forces of dielectric liquid can enter the vicinity of EDM spot to remove the melted material.

One of the most recognized model of EDM process, the Van Dijck's one, highlights that boiling is the main mechanism of material removal. This occurs just after the pulse end due to overheated material with around 200-

300 K over boiling point due to sudden fall of the pressure around EDM spot [6].

The validation of this model was accomplished only after the ultra speed cameras with more than 10^6 frames/s were used which allowed the micrometric scale phenomena observation from the working gap. Thus, Schulze et al. emphasized that when using working parameters compatible to micromachining, e.g. 1 A discharge current, 15 μm working gap and 10 μs pulse time, the gas bubble was in the gap even after 120 μs from the pulse end [7].

The generic evolution of such gas bubble at micromachining is described in fig.1:

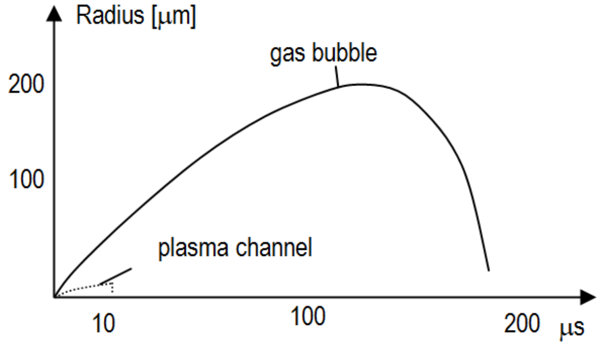

Fig.1. Plasma channel and gas bubble qualitative evolution at micromachining.

During real machining process, the next discharge - which depends on delay time (t_d) - is able to determine the collapse of the gas bubble produced by previous discharge. In case of μEDM, according to our experiments, t_d is relative long, more than 100 μs due to low electrical conductivity. This is the result of low discharge energy, specific to micromachining [2]. Under these circumstances, as FEM modelling will emphasize, the melted material is long time ago resolidified and cannot be removed by hydraulic forces by the moment of gas bubble implosion. Thus, at classic μEDM, the main mechanisms of material removal remain the boiling after the pulse end and evaporation during pulse time.

At μEDM+US, the material removal mechanism is very much affected by cavitational phenomena, specific to semiperiods of ultrasonic longitudinal oscillations of electrode-tool (fig.2). In the first one, compression of dielectric liquid from the gap is produced and in the second one, the liquid stretching is determined by variation of total hydraulic pressure. Since the working gap has micrometric dimensions, the liquid compression and stretching are facilitated by capillary phenomena.

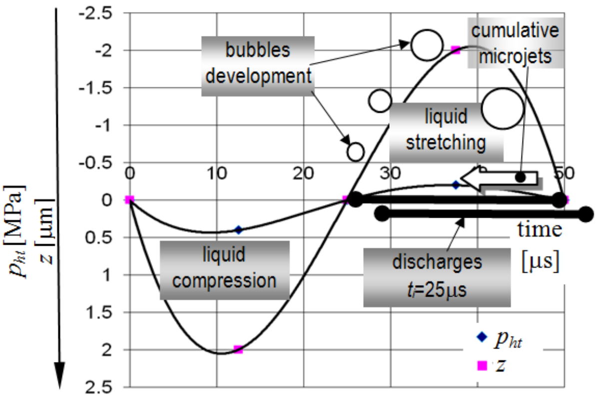

Fig.2. *Variation of total hydrostatic pressure (p_{ht}) along of tool elongation (z) in the frontal gap at μEDM+US.*

The total hydraulic pressure (p_{ht}) is determined by the relation:

$$p_{ht} = 2\pi \cdot c \cdot \rho \cdot f_{US} \cdot A \sin \omega t + p_h \quad \text{[MPa]} \quad (1)$$

where: c is sound velocity in dielectric liquid [m/s]; ρ - density of dielectric liquid [kg/m^3]; f_{US} - ultrasonic frequency [Hz]; A - oscillation amplitude [m]; $\omega=2\pi f_{US}$ [s^{-1}]; p_h - local hydraulic pressure from the gap [MPa].

The pressure variation from fig.2 was achieved when working with dielectric liquid with ρ=840 kg/m^3 ; f_{US}=20kHz, A=2μm p_h was considered 0.1 MPa. Under these working conditions, cavitation was obtained.

At each final stretching semiperiod, that lasts 25 μs in this case, collective implosion of bubbles from the gap is produced due to p_{ht} increase (cumulative microjets stage). Huge pressure of 10 MPa order is developed and shock waves parallel to machined surface decrease roughness by removing micropeaks with low shear resistance.

3. EXPERIMENTAL DATA

Some reference experimental data for FEM modelling validation - obtained when machining X210Cr12, tool steel, on Romanian ELER 01 machine with commanded pulses, current step I=0.8A, pulse time t_i=25μs, pause time t_0= 12μs, positive polarity - were synthesized in table 1. The output main parameters of micromachining when static pulse durations are used are presented in fig.3.

Table 1. Craters mean dimensions

Machining	EDM		EDM+US	
Crater dimensions	Depth [μm]	Radius [μm]	Depth [μm]	Radius [μm]
	3.6	5.5	1.8	3.5

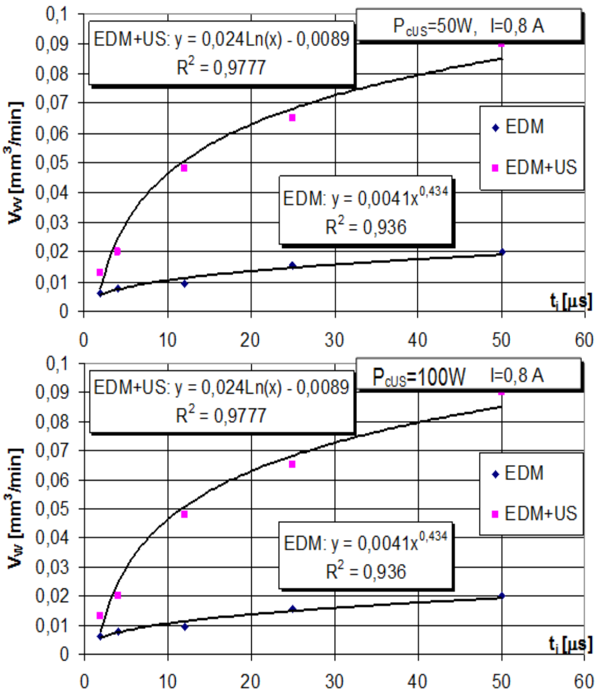

a) Machining rate versus pulse time

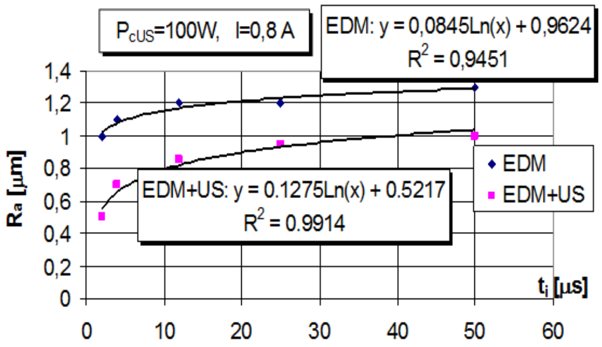

b) R_a roughness versus pulse time

Commanded pulses; workpiece - X210Cr12; ϕ 30 flat electrode - Cu 99.5; dielectric liquid 840 kg/m^3

Fig.3. Machining rate improving by ultrasonic aided EDM.

It can be noticed that machining rate increase is more apparent at longer pulse time (more than 12 μs) and R_a roughness decrease is more visible at shorter pulse time (lower than 12 μs).

3. FEM MODELLING

The removal mechanism through commanded pulses was approached, obtaining temperature distribution after pulse end, after bubble collapse and at cumulative microjets stage (fig.2); thus, the modelling addresses the synchronization between electrical discharges and the ultrasonic elongation of electrode-tool.

The 2D geometry was created, due to the symmetry of approached phenomena aiming at computational resource saving (fig.4). The workpiece was a 10 mm square; from fig.7, it can be noticed that dimensions of 10 mm order have no influence on FEM results. The EDM spot was applied on initial surface with craters produced by previous discharges. Major errors are produced in terms of crater dimension modelling when initial surface is flat [2].

Thus, the current EDM spot was applied on the symmetry axis of microgeometry, comprising two adjacent previous craters, on the interval x=[-5.5;5.5] μm. The geometry shape takes into account the specificity of static pulse duration form with material resolidified on crater border – semicircles of 0.5 μm diameter - due to difficult evacuation from a deep molten volume [1].

The extension of gas bubble of 0.2 mm diameter formed around plasma channel was defined by PT1 and PT2 points, placed on the superior surface of the workpiece.

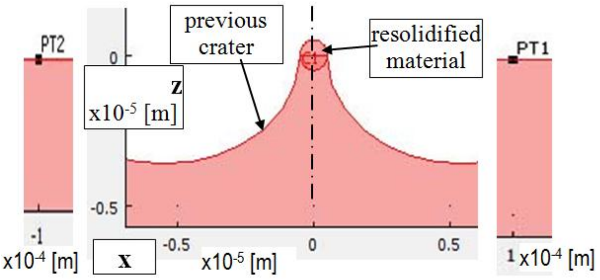

Fig.4. 2D geometry parameters.

Meshing was based on Lagrange-T_2J_1 triangular elements with statistics presented in fig.5. As one can see, due to a finer meshing in the zone adjacent to EDM spot, which will be thermally affected by discharge, the meshing quality on the scale 0-1 is over 0.85. Aiming at computational resource saving, the meshing is ordinary on the rest of workpiece volume without influencing the results.

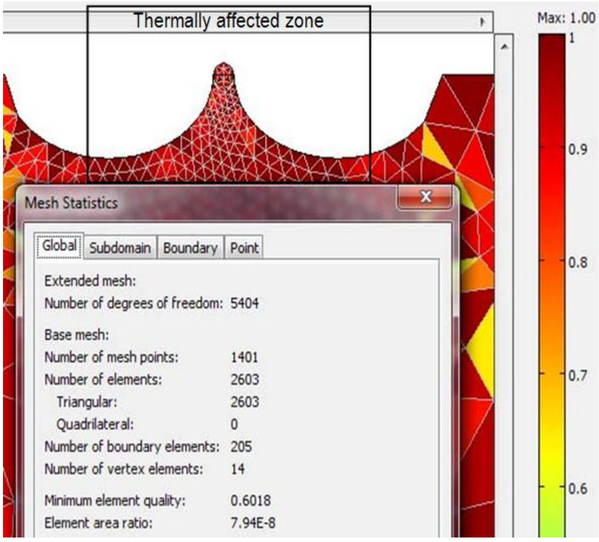

Mesh Statistics

Extended mesh:
Number of degrees of freedom: 5404

Base mesh:
Number of mesh points: 1401
Number of elements: 2603
Triangular: 2603
Quadrilateral: 0
Number of boundary elements: 205
Number of vertex elements: 14

Minimum element quality: 0.6018
Element area ratio: 7.94E-8

Fig.5. Meshing close to EDM spot.

Thermal properties of X210Cr12 (D3 DIN) were loaded from Comsol Multiphysics library, all of them being temperature dependent.

For boundary settings, EDM spot was put at 3475K (fig.6) taking into account the assumption that during the pulse time the melted material is overheated above boiling temperature (around 3000 ^{o}C at steel) with 200^{o}C due to increased pressure produced by plasma channel [6]. The adjacent zones to EDM spot, bordered by PT1 and PT2 were considered as insulated due to gas bubble influence. The rest of boundaries belonging to workpiece were set at dielectric liquid temperature, which generally is 313 K.

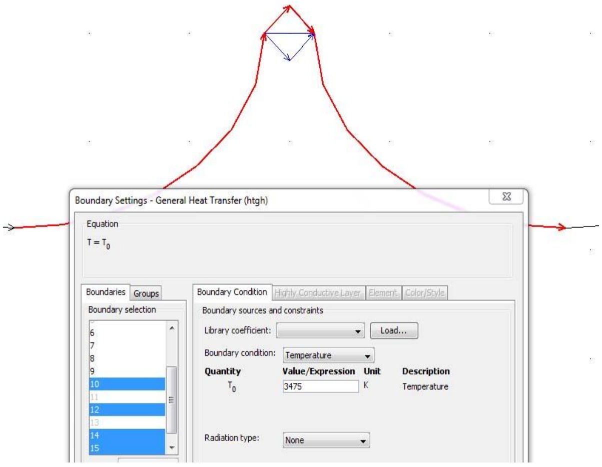

Boundary Settings - General Heat Transfer (htgh)

Equation

$T = T_0$

Boundary selection

Boundary sources and constraints

Library coefficient:

Boundary condition: Temperature

Quantity	Value/Expression	Unit	Description
T_0	3475	K	Temperature

Radiation type: None

Fig.6. Boundary conditions on EDM spot zone.

At classic μEDM, the modelling cycle comprised heating by 25 μs pulse time (t_i), followed by 100 μs cooling time interval until next discharge occurs.

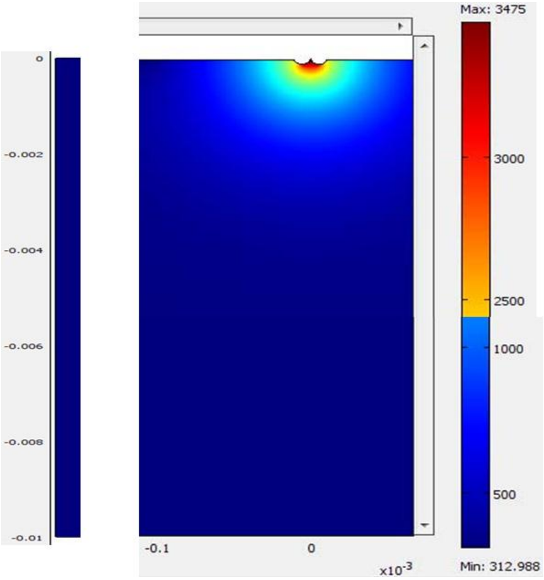

Fig.7. Thermal distribution after 25 μs static pulse duration on workpiece volume.

The FEM first results highlight that a very small part of the workpiece (of mm order) is thermally affected by 25 μs discharge (fig.7). In detail, the crater depth is located at z=3.8 μm and radius x=5.8 μm given by boiling isothermal (3273 K) position under normal conditions, after pulse end (fig.8). These results are within 5% margin against experimental data and thus the validation of the model could be considered.

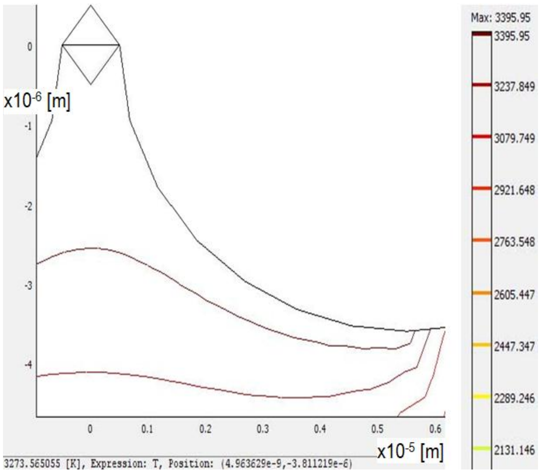

3273.565055 [K], Expression: T, Position: (4.963629e-9,-3.811219e-6)

Fig.8. Thermal distribution after 25 μs static pulse duration close to EDM spot.

The remaining material after discharge removal modelling suffers 100 μs cooling. The temperature distribution is presented in fig.9, pointing out that its maximum temperature is around 374 K. Thus, no volume could be removed by hydraulic forces of dielectric liquid because by the time of bubble implosion, due to next discharge occurring, the melted material was long time ago resolidified. The melting point of steel with 2.1 % C and 12% Cr is 1683K.

Moreover, analyzing the temperature evolution in the point of coordinates [x,z] = [0,-4.4] μm, one can notice the following evolution of temperature (fig.10): just after the pulse end at the beginning of cooling, the temperature was around 3200K (liquid state); after 100 μs, the point temperature was 374 K; the temperature decrease is very fast, so after approximately 1.5 μs, the temperature was under 1683K (solid state).

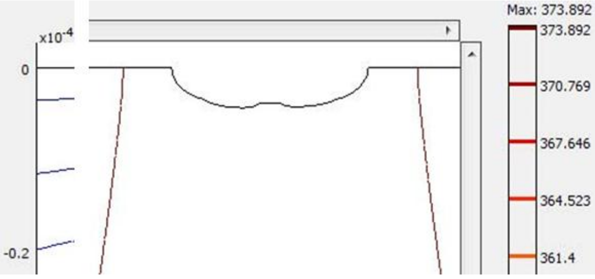

Fig.9. Thermal distribution after 100 μs from the pulse end close to EDM spot.

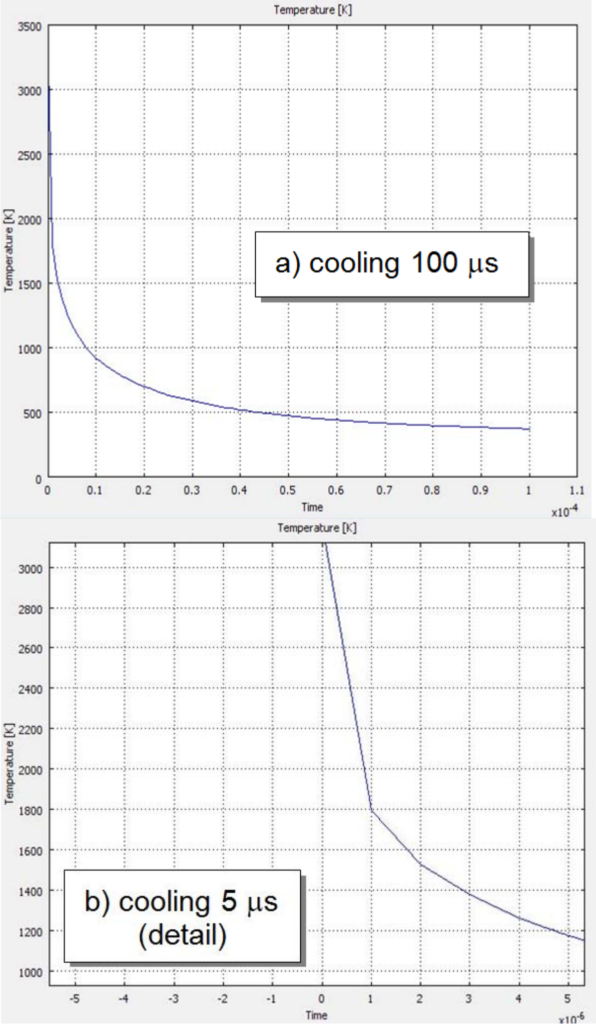

Fig.10. Temperature evolution at 100 μs cooling in the point [0,-4.4] μm.

Therefore, at EDM+US, if the dielectric liquid can reach the EDM spot in less than 1.5 μs after the pulse end, through gas bubble implosion, it can remove some melted material. This synchronization between pulse end and cumulative microjets stage (stretching semiperiod stage) is very difficult to achieve in such a short margin. However it can produce huge enhance of volume removed by discharge given by melting isothermal of 1683K (fig.11).

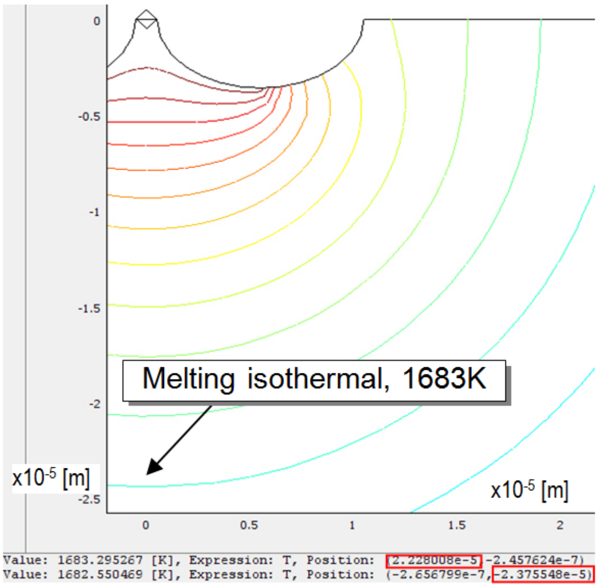

```
Value: 1683.295267 [K], Expression: T, Position: (2.228008e-5,-2.457624e-7)
Value: 1682.550469 [K], Expression: T, Position: (-2.656799e-7,-2.375548e-5)
```

Fig.11. Melting isothermal 1683K position after 25 μs static pulse duration.

The position of melting isothermal is defined by its radius and depth, [x=22μm; z=23μm] coordinates indicated at bottom of fig.11. Comparing the volume of this half-ellipsoid with the corresponding one resulted from classic EDM, it results that US aiding can produce more than 90 times, increase of removed volume by single discharge. Then the FEM study was focused on overlapping of pulse time on collective bubble implosion, obtaining temperature distribution after 5 (fig.12), 3 (fig.13), and 2 μs (fig.14), from the pulse beginning, based on the hypothesis that cumulative microjets stage allows the access of dielectric liquid to melted material.

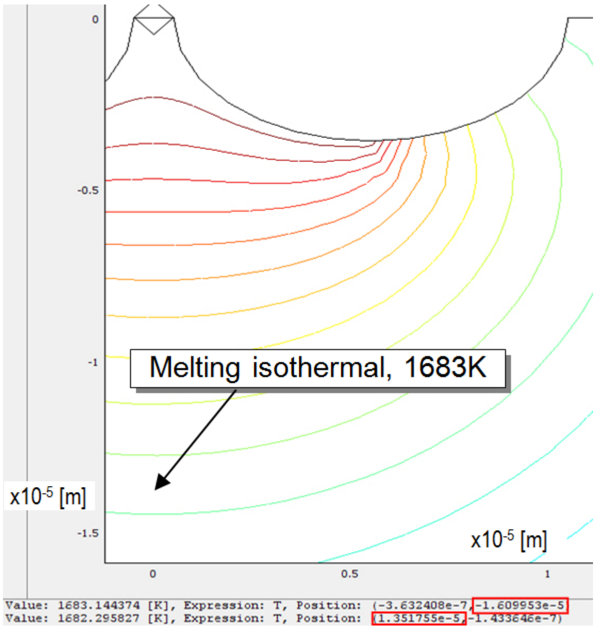

```
Value: 1683.144374 [K], Expression: T, Position: (-3.632408e-7,-1.609953e-5)
Value: 1682.295827 [K], Expression: T, Position: (1.351755e-5,-1.433646e-7)
```

Fig.12. Melting isothermal 1683K position after 5 μs from pulse beginning.

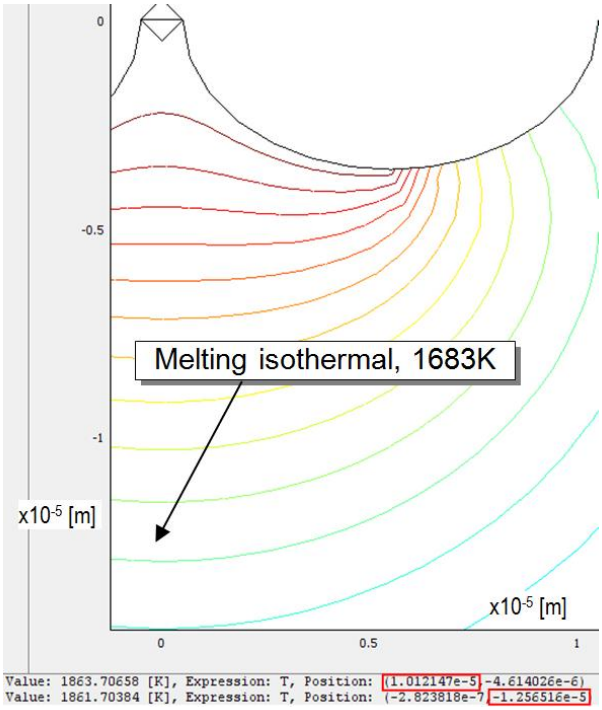

```
Value: 1863.70658 [K], Expression: T, Position: (1.012147e-5,-4.614026e-6)
Value: 1861.70384 [K], Expression: T, Position: (-2.823818e-7,-1.256516e-5)
```

Fig.13. Melting isothermal 1683K position after 3 μs from pulse beginning.

The temperature distributions pointed out that a small overlapping of bubble collective implosion, even of 2 μs from pulse beginning, could increase the volume removed by single discharge up to 8 times (fig.14). Overall, this synchronization is able to amazingly increase the machining rate. Nevertheless, the EDM+US experimental data from table 1 show that crater dimensions are lower than at classic EDM. This could be the effect of cumulative microjets oriented parallel to machined surface, which can remove the margins of the crater, reducing the depth and the radius, and implicitly the R_a roughness.

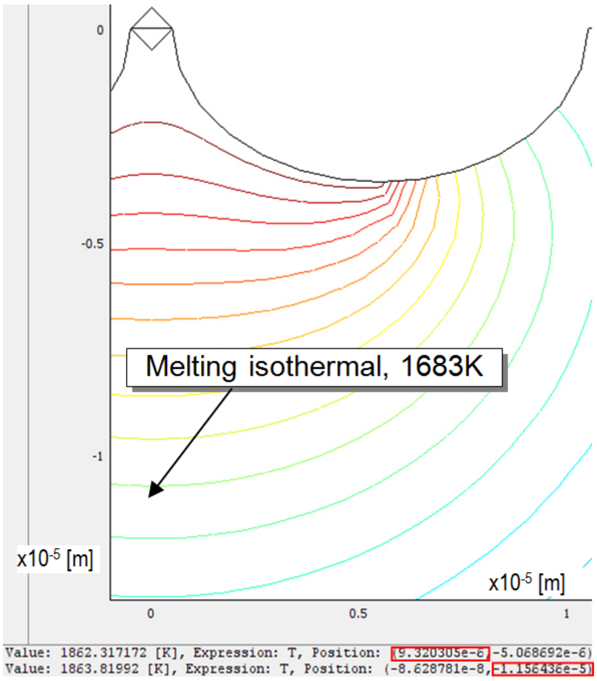

```
Value: 1862.317172 [K], Expression: T, Position: (9.320305e-6,-5.068692e-6)
Value: 1863.81992 [K], Expression: T, Position: (-8.628781e-8,-1.156436e-5)
```

Fig.14. Melting isothermal 1683K position after 2 μs from pulse beginning.

4. CONCLUSIONS

From experimental data confirmed by FEM modelling, it results that working with longer pulse time (25 μs) the advantage of US aiding of μEDM is more apparent in terms of machining rate. This is based on synchronization of bubbles collective implosion ultrasonically induced with pulse time: either bubble collective implosion falls within the pulse time (more probable to achieve) or very close to its end (technically very difficult). FEM results emphasized that potential of machining rate increase of μEDM+US is very huge at longer pulse time. Since the main objectives are high precision of fine details and surface quality, longer pulse time than 25 μs are not appropriate at usual 20 kHz frequency due to higher pulse energy.

Acknowledgment: These paper results belong to CNMP Partnership project, 72-194.

REFERENCES

[1] GHICULESCU, D., Nonconventional Machining, Printech, Bucharest, 2004.

[2] GHICULESCU, D., et al. Finite element analysis of gas bubble influence on ultrasonic aided electrodischarge machining. Proceedings of the 7th International DAAAM Baltic Conference Talinn, Estonia, pag. 177-182, 2010.

[3] HUANG, H. et al., Ultrasonic vibration assisted electro-discharge machining of microholes in Nitinol, J. Micromech. Microeng., 13 693-700, 2003.

[4] HUNG, J.-C. et al., Using a helical micro-tool in micro-EDM combined with ultrasonic vibration for micro-hole machining, Journal of Micromechanics and Microengineering, pag. 2705-2713, Vol. 16, 2006.

[5] MARINESCU, N.I., GHICULESCU, D., et al., Tehnologii cu energii concentrate pentru micro si nanostraturi, Printech, Bucharest, 2008

[6] VAN DIJCK, F., SNOEYS, R., Theoretical and Experimental Study of the Main Parameters Governing the Electrodischarge Machining Process*, Mecanique*, Vol. 301-302, p. 9-16. 1975.

[7] SCHULZE, H.-P. et al., Gas bubble morphology in small working gaps at spark erosion, 2004, *Available from:* http://eco.pepublishing.com/ *Accessed:*2010-09-5.